Universitetet i Stavanger

FACULTY OF SCIENCE AND TECHNOLOGY

BACHELOR'S THESIS

Study programme/specialisation:	Spring semester, 2024
Computer Science	Open /~~Confidential~~

Authors: Haakon Volheim Webb, Håkon Nodeland, William Vagle
Programme coordinator: Naeem Khademi

Supervisor(s): Naeem Khademi

Title of Bachelor's Thesis: Bluetooth-based Vehicle and Pedestrian Positioning for Road Tunnels: A Performance Evaluation Study

Credits: 20

Keywords:	Pages: 44
BLE, Positioning, Tunnel, RSSI	+ attachments
	Stavanger 15. mai 2024

Contents

Abstract

The capability and demand of locating devices in any environment are anticipated to rise. This is also true for autonomous vehicles, Vehicle-to-Everything systems, and emergency services. Today's solutions with the Global Navigation Satellite System (GNSS) and dead-reckoning become lackluster when inside of tunnels. Bluetooth Low Energy (BLE) serves as an alternative to this problem with its affordable prices and scalability in terms of maintenance and installment. This project's main focus is BLE-based positioning of vehicles and pedestrians inside of road tunnels.

Most of the available work related to Indoor Positioning System (IPS) is focused on the indoor scenario. With the small amount of research into how these IPSs perform inside of tunnels, it becomes unclear how they will perform in that environment.

This thesis will therefore take the experimental approach to measure the performance of a BLE RSSI-based IPS in a tunnel scenario, where you can have both pedestrians and vehicles traveling at high speeds.

Experiments were conducted in a tunnel located in Skaarlia, Sandnes. Even with the use of high-end equipment, it was concluded that the evaluated algorithms did not perform better than GNSS.

Preface

This thesis was written at the University of Stavanger for the department of Electrical Engineering and Computer Science.

We would like to thank our supervisor, Associate Professor Naeem Khademi, for outstanding guidance and excellent feedback. Your enthusiasm for the problem was inspiring, and your knowledge of the field motivating.

Also, we would like to thank Aitor Martin Rodriguez for supplying us with the OBU, and guidance on how we could perform the tests in the tunnel, and also explaining the problem of signal propagation to give us a better understanding. We wish you the best of luck on your PhD work.

Special thanks to Arkadiusz Benicki from Sandnes Kommune for supplying the drawings related to the tunnel in Skaarlia and coordinating how we could go forward with our experiments in a safe manner.

Thanks to Ståle Freyer for granting access to the lab so we could make the OBD connector for the OBU that we used in our experiments, and also for providing us with new batteries for the beacons.

Acronyms

AoA Angle of Arrival

BLE Bluetooth Low Energy

dBm Decibel-milliwatt

E Empirical

EID Ephemeral Identifier

GNSS Global Navigation Satellite System

IPS Indoor Positioning System

ITU International Telecommunication Union

LDPL Log-Distance Path Loss

LoS Line of Sight

MAC Media Access Control

MCPD Multi Carrier Phase Difference

N/A Not Applicable or Not Available

OBU On-board Unit

OS Operating System

RSSI Received Signal Strength Indicator

Rx Received Level

SDOR Single Direction Outlier Removal

SMA Simple Moving Average

Tx Transmitted Level

TLM Telemetry

UID Unique Identifier

UiS University of Stavanger

URL Uniform Resource Locator

UUID Universally Unique Identifier

V2X Vehicle-to-Everything

WMA Weighted Moving Average

Chapter 1

Introduction

Indoor positioning is a rapidly evolving sector, with many innovative solutions for buildings, malls, stores and public areas. However, there is still a lack of accurate positioning systems for tunnels. The portion of the road network in Norway that is inside of tunnels represent a total of 1550km [1]. Therefore, installing equipment requires low maintenance and preferably low cost.

With Bluetooth-based positioning being widely explored in other areas, it is worth exploring if it can provide accurate results for tunnels as well.

1.1 Motivation

As of 2022, Norway has over 1260 active tunnels in its road network [1]. As newer tunnels are made, the focus on safety has been prioritized. For instance, the Ryfast tunnel in Stavanger has cameras installed [2]. The cameras can be used to view the inside of the tunnel, and provide the observer with localizations of objects inside of it. This can aid emergency personnel in the case of a road accident. However, older tunnels have little to no technology or infrastructure for emergency detection or localization of cars and pedestrians.

A problem both newer and older tunnels share is that they have no line of sight (LoS) to the GNSS. As the GNSS signals fail to penetrate tunnel walls, most vehicles and devices rely on dead reckoning, which is a method to continue to estimate one's position when the GNSS signals fade. The position is calculated via the object's Inertial Movement Unit (IMU)[3], which provides information on acceleration and orientation to name a few [4]. Using dead reckoning can quickly accumulate errors, and without the GNSS to correct these errors, the object's position estimation becomes unreliable. Consequently, an improvement to the currently used dead reckoning approach is needed for the tunnel scenario.

The need for continuous and precise location information is becoming essential. This increasing need is particularly highlighted in sectors such as autonomous vehicle navigation, Vehicle-to-Everything communication (V2X) and emergency services, amongst others. Emergency services need to be able to tell where injured people are located to safely evacuate and rescue them, and autonomous vehicles need to be able to safely navigate the tunnels. Infrastructure and solutions for positioning must therefore evolve in order to keep up with the demand.

Bluetooth Low Energy (BLE) is already deployed in public and private areas around the world. BLE can be seen in malls to provide nearby devices with information regarding special offers [5]. A BLE-based IPS is a low cost, low maintenance system that stands out as a solution to the current issues that tunnels face. They provide cheap infrastructure, which can be used for the positioning of objects. Maintaining the infrastructure is simple because it is easy to access and because of the lifetime of the beacons' internal batteries.

1.2 Problem Statement

Many different underlying technologies exist that can support an IPS. Table 1.1 gives an overview of several popular IPS implementations and provided a perspective on the accuracy of them. An indication to the cost of the implementations has been provided as well [6]. All of the papers referenced in the table, conducted their experiments in an indoor scenario. There are no performance evaluations of an IPS in the tunnel environment.

Underlying Technology	Accuracy	Cost	Reference
BLE AoA	0.6m	Low	[7]
BLE RSSI	1.8m	Low	[8]
Computer Vision	1.4m	Medium	[9]
Magnetic Field	0.55m	Low	[10]
Ultra-Wideband	0.2m	High	[11]
Wi-Fi AoA	0.33m	No additional cost (indoor)	[12]
Wi-Fi RSSI	1.05m	No additional cost (indoor)	[13]

Table 1.1: Comparison between underlying technology, accuracy and cost.

A BLE RSSI-based IPS implementation has been developed for the tunnel scenario [14]. In their implementation, the beacons were placed with 40 meters intervals, and a proximity approach was used. The position of an object was given by the beacon closest to the object. This presented great promise to replace dead reckoning, but they did not implement any other algorithms.

Another paper focused on the tunnel scenario was presented in [15]. They attempted to locate mobile devices in a tunnel, and to guide the users to the nearest exit using RSSI.

This then leaves a gap in the current research related to IPS using BLE in road tunnels. There are several questions to be addressed: Which of these algorithms are more effective for tracking a vehicle, and which algorithms are more effective for tracking a pedestrian? To what extent will the accuracy of the various algorithms play a role for the different scenarios?

To further address the problem, three research questions are formulated:

Q1: Which algorithm has the highest accuracy in a dynamic scenario?

Q2: Which algorithm has the highest accuracy in a static scenario?

Q3: Will this approach improve accuracy over current solutions?

1.3 Objective

The primary objective is to find the best algorithm for positioning inside of tunnels. Several algorithms, some that has been used by others and one that has not, will be evaluated for three different scenarios. A comparison of all algorithms will be presented, and best performing algorithm will be found.

For the static scenario, inside a tunnel where visibility might be obscured for emergency personnel, the accuracy of the algorithm is not as heavily weighted, as opposed to its reliability. However, while tracking the location of a car in motion, a greater accuracy is required for the positioning to be precise at higher speed.

1.4 Approach

The research approach that has been performed in this thesis, are experimental efforts. There have been several experimental scenarios. These have been conducted in both controlled and uncontrolled environments, and in crowded and less populated areas, for both static and dynamic scenarios.

1.5 Background

The foundation of BLE-based Indoor IPSs are Received Signal Strength Indicator (RSSI) and signal propagation models. RSSI refers to the strength of a signal when captured by a receiving device. Signal propagation models refers to mathematical models that simulate the natural reduction in signal strength as the distance between source and receiver increases. Trilateration is the principle of finding the coordinates of an unknown point using the distances from the unknown point to three known reference points.

1.6 Thesis Outline

The thesis is structured as followed:

Chapter 2 - Related Work: This chapter introduces similar research that has been done by other authors. It also extracts algorithms that will be used to estimate positions in later chapters.

Chapter 3 - Research Method: This chapter goes over what tools were used to accommodate the experimental approach of the thesis.

Chapter 4 - Experimental Setup: Public bus rides and the Skaarlia tunnel were used in the experimental approach. This chapter shows the experimental setup in these environments.

Chapter 5 - Experimental Results: The results from the public bus rides and the Skaarlia tunnel are displayed graphically.

Chapter 6 - Discussion: The results from the previous chapter is discussed and compared to technologies.

Chapter 7 - Conclusion: A conclusion is drawn based on the formulated research questions and future work is discussed.

Chapter 2

Related Work

There are different ways to solve indoor positioning. BLE RSSI-based [16], Wi-Fi RSSI-based [17], Ultra-Wideband [18], Magnetic Fields or Computer Vision can be used [19] [20]. A thorough meta-review from 2019 evaluated the advancements of all the different IPS solutions in the field, for all previously mentioned techniques, and more, from 2015 to 2019 [21]. For BLE RSSI-based IPSs, the typical error was reported to be 2-5 meters. None of the papers referenced in the review analyzed the performance of an IPS inside of tunnels.

In 2017, a comparison of the performance of several algorithms based on channel diversity for RSSI was conducted, as well as three different signal propagation models [16].

A hybrid approach combining Wi-Fi and BLE was suggested in 2018 [22]. After comparing the accuracy of the two different IPSs, their experiments showed that the BLE-based solution performed better in more beacon dense areas, with a lower error rate. However, as distances grew the accuracy diminished unlike Wi-Fi. Therefore, a unified approach was proposed.

In 2020, a BLE RSSI-based IPS solution was developed, with a reported median accuracy of 1.72 meters for their static experiment [8]. They compared how raw RSSI signals performed against both filtered values, a minimum RSSI threshold and a centroid calculation based on previously calculated

points.

In 2022, the accuracy of a non-linear RSSI-based algorithm was compared to the accuracy of an AoA approach [23]. It was concluded that the mean error for the AoA approach was lower than that of the RSSI-based algorithm. As mentioned earlier, the only available papers regarding the implementation of an IPS inside of a tunnel was published in 2023 [14]. A real, functioning IPS solution was implemented for the entire length of a tunnel.

Underlying Technology	Average Error	Reference
BLE RSSI	1.8m	[8]
BLE RSSI	0.3m	[24]
BLE RSSI	1.6m	[25]
BLE RSSI	4.6m	[16]
BLE RSSI	7.1m	[23]
BLE AoA	1.4m	[23]
BLE AoA	0.6m	[7]
BLE AoA	0.14m	[26]

Table 2.1: Comparison of different implementations that has been used and their accuracy.

2.1 RSSI-Based Algorithms

RSSI-based algorithms refers to the algorithms that an RSSI-based IPS can utilize. Any RSSI-based IPS has three components. The RSSI filter, which is applied to reduce the variance from the incoming RSSI measurements. Furthermore, a distance estimation algorithm is responsible for converting the RSSI values to meters. Moreover, a positioning algorithm uses the distances generated by the distance estimation algorithms to calculate a position in the plane.

2.1.1 RSSI Filter: Single Direction Outlier Removal

The single-direction outlier removal (SDOR) algorithm filters out high-deviance values. RSSI tends to decline due to indoor multi-path fading

[24]. The purpose of this filter is to remove these RSSI values. In the algorithm, for each RSSI value captured, n of the most recent RSSI values are stored, where n is the window size of the filter, and the newly captured RSSI value is the last entry of $RSSI_{Recent}$. Mean, $RSSI_{mean}$, and standard deviation, $RSSI_{SD}$, are calculated from the n recent RSSI values. Outliers are then removed using the following logic:

$$RSSI_{Recent} = \begin{cases} \text{remove} & \text{if } RSSI_i \leq RSSI_{mean} - C_{SD} \cdot RSSI_{SD} \\ \text{include} & \text{otherwise} \end{cases} \tag{2.1}$$

Where C_{SD} represents the standard deviation coefficient. Its magnitude determines the level of filtration, with a higher coefficient providing more filtration.

Then, the average RSSI value from the remaining entries in $RSSI_{recent}$ is the RSSI value that the filter saves from the newly captured measurement.

Window sizes n of both 10 and 20 has been used, as well as standard deviation coefficients C_{SD} of 2 and 1.2 [24], [27].

2.1.2 RSSI Filter: Moving Average

Another approach to reduce the signal noise of the measured RSSI is to implement a moving average. A Simple Moving Average (SMA) and Weighted Moving Average (WMA) has been previously utilized for a BLE-based IPS [8]. The equations for these are as followed:

$$SMA = \frac{RSSI_0 + RSSI_1 + ... + RSSI_{n-1}}{n} \tag{2.2}$$

$$WMA = \frac{n \cdot RSSI_0 + (n-1) \cdot RSSI_1 + ... + RSSI_{n-1}}{1 + 2 + ... + (n-1) + n} \tag{2.3}$$

Where $RSSI_0$ is the most recent RSSI value captured and n is the window size.

The difference between the two algorithms is how each individual measurement is weighted. For SMA, the most recently captured measurement is

weighted the same way as the oldest measurement in the window, at $\frac{1}{n}$. WMA however, applies different weights to all measurements. The most recent measurement is weighted by $\frac{n}{1}$, while the last is weighted by $\frac{1}{n}$.

2.1.3 Distance Estimation: Empirical Model

The Empirical Propagation Model (E) is a commonly used model [8]. The model estimates the distance based on two parameters, and is given as:

$$RSSI = -10\gamma log_{10}(d) + A \tag{2.4}$$

Firstly, the path loss exponent, noted as γ, refers to the loss of the strength of a signal, propagating through a given environment. This parameter is usually in the 2-4 range, and needs to be configured for each environment individually:

$$\gamma = \frac{A - RSSI}{10log_{10}(d)} \tag{2.5}$$

The second parameter A, the Tx-power, represents the signal strength measured at a distance of 1 meter away from the transmitting device. The Empirical model is given in equation 2.6. Where RSSI is the RSSI value chosen to estimate distance.

Which can be solved for the distance d as followed:

$$d = 10^{(\frac{A-RSSI}{10\gamma})} \tag{2.6}$$

2.1.4 Distance Estimation: Log-Distance Path Loss Model with Shadowing

The Log-Distance Path Loss model (LDPL) is the second propagation model tested [16]. It is given by:

$$RSSI = A + 10(\frac{d}{d_0}) + X\sigma \tag{2.7}$$

Where A is the RSSI captured at the reference distance d_0, which usually is 1 meter. γ is the path loss-exponent and $X\sigma$ is the zero-mean Gaussian

distributed random variable with standard deviation. The $X\sigma$ parameter is used to attempt to compensate the random shadowing effect, and is set to 3.2 [28].

The equation can be solved for the distance d:

$$d = d_0 10^{(\frac{\text{RSSI}-\text{RSSI}(d_0)-X\sigma}{10n})} \tag{2.8}$$

2.1.5 Distance Estimation: The ITU Model for Indoor Environments

Additionally, the International Telecommunication Union model for indoor attenuation (ITU) has been implemented [16]. It has the following equation:

$$L_{Total} = 20logf + Nlog(d) + P_f(n) - 28 \tag{2.9}$$

Where L_{total} is the total loss in signal strength, f is the frequency in MHz, N is the distance power loss coefficient and $P_f(n)$ is the floor loss penetration factor. The variables N and $P_f(n)$ can be chosen by following ITU's recommendations. The equation can be solved for the distance d:

$$d = 10^{(\frac{\text{RSSI}_0-\text{RSSI}+28-P_f(n)-20\log f}{N})} \tag{2.10}$$

2.1.6 Trilateration Algorithm: Matrix Product

The foundation of all the following trilateration algorithms, is the circular equation:

$$r^2_{a,b,c} = (x - x_{a,b,c})^2 + (y - y_{a,b,c})^2 \tag{2.11}$$

Equation 2.11 can be rearranged to form the following trilateration algorithm:

$$\begin{bmatrix} x \\ y \end{bmatrix} = \begin{bmatrix} A_1^2 + A_2^2 + A_3^2 & A_1B_1 + A_2B_2 + A_3B_3 \\ A_1B_1 + A_2B_2 + A_3B_3 & B_1^2 + B_2^2 + B_3^2 \end{bmatrix} \times \begin{bmatrix} A_1 + C_1 + A_2C_2 + A_3C_3 \\ B_1C_1 + B_2 + C_2 + B_3C_3 \end{bmatrix} \tag{2.12}$$

Where $A_{1,2,3}$, $B_{1,2,3}$, $C_{1,2,3}$, refers to the different relationships between anchor points and radii. All the details of this algorithm can be found in [29].

2.1.7 Trilateration Algorithm: Determinants

Another trilateration algorithm was derived in [16]. This is also derived from equation 2.11.

$$x = \frac{\begin{vmatrix} (r_a^2 - r_b^2) - (x_a^2 - x_b^2) - (y_a^2 - y_b^2) & 2(y_b - y_a) \\ (r_a^2 - r_c^2) - (x_a^2 - x_c^2) - (y_a^2 - y_c^2) & 2(y_c - y_a) \end{vmatrix}}{\begin{vmatrix} 2(x_b - x_a) & 2(y_b - y_a) \\ 2(x_c - x_a) & 2(y_c - y_a) \end{vmatrix}} \tag{2.13}$$

$$y = \frac{\begin{vmatrix} 2(y_b - y_a) & (r_a^2 - r_b^2) - (x_a^2 - x_b^2) - (y_a^2 - y_b^2) \\ 2(y_c - y_a) & (r_a^2 - r_c^2) - (x_a^2 - x_c^2) - (y_a^2 - y_c^2) \end{vmatrix}}{\begin{vmatrix} 2(x_b - x_a) & 2(y_b - y_a) \\ 2(x_c - x_a) & 2(y_c - y_a) \end{vmatrix}} \tag{2.14}$$

2.1.8 Trilateration Algorithm: System of Equations

The final trilateration algorithm that has been evaluated is given by the following [30]:

$$x = \frac{CE - FB}{EA - BD}$$
$$y = \frac{CE - FB}{BD - AE} \tag{2.15}$$

Where

$$A = (-2x_a + 2x - b)$$
$$B = (-2y_a + 2y_b)$$
$$C = r_a^2 - r_b^2 - x_a^2 + x_b^2 - y_a^2 + y_b^2$$
$$D = (-2x_b + 2x_c)$$
$$E = (-2y_b + 2y_c)$$
$$F = r_b^2 - r_c^2 - x_b^2 + x_c^2 - y_b^2 - y_c^2$$

2.2 Noteworthy Algorithms

Several papers discuss how a Kalman Filter is applied to the position estimations to improve the accuracy of their results [24], [16], [27], [31]. For all scenarios and use cases, the Kalman Filter increases accuracy. The benefit of the Kalman Filter is clearly documented. It is a filter which is applied as a final adjustment to the positioning estimations themselves, at the very end of the process. Consequently, it was decided that the Kalman Filter would be omitted from the comparison provided here.

A new ranging technique that was introduced with Bluetooth 5.1 was Multi-Carrier Phase Difference (MCPD), which is based on AoA [32]. A comparrison of MCPD- and RSSI-based indoor localization systems revealed MCPD's superior accuracy [33]. The study highlights the potential of MCPD with its mean error of 0.50m, compared to RSSI's 1.39m mean error. It significantly outperforms RSSI and it truly highlights the potential this technique has for precise indoor positioning. However, due to the lack of equipment to support the multiple antenna array, the AoA-based approach has not been included in the comparison.

2.3 Beacon Protocols

There are several different protocols for beacons. The two most commonly used are iBeacon and Eddystone. iBeacon is a technology made by Apple and it was the first BLE protocol to be released in 2013 [34]. Eddystone is a Google-developed protocol for BLE beacons that was released in 2015. Unfortunately, it failed only three years later [35]. While iBeacon is a closed proprietary standard, Eddystone is open-source and multi-platform, which means that both iOS and Android devices can use the standard.

2.3.1 iBeacon

iBeacon broadcasts four frames [34]:

1. UUID, to identify the beacon.
2. Major, a number to identify a subset of beacons within a large group.
3. Minor, a number to identify a specific beacon.
4. Tx power level, indicating the signal strength one meter from the device. This must be calibrated by the user or manufacturer.

2.3.2 Eddystone

Eddystone also has the availability to broadcast four frames [35]:

1. URL, broadcasts a URL that other Bluetooth-enabled devices can see.
2. UID, transmits a short id code time and again.
3. TLM, sends telemetry data reading the beacons status and attached sensors.
4. EID, a security layer that is added.

2.4 Scope of the Thesis

The scope of the thesis is to provide a performance evaluation between different algorithms combined with different filters. The different filters and algorithms are as follows:
The RSSI-filters.

1. Single Direction Outlier Removal (SDOR) 2.1
2. Simple Moving Average (SMA) 2.2
3. Weighted Moving Average (WMA) 2.3

Which will all be used in combination with three different Distance Estimation algorithms.

1. Emperical Propagation Model (E) 2.6
2. Log-Distance Path Loss with Shadowing (LDPL) 2.8
3. The International Telecommunication Union's Propagation Model for Indoor Environments (ITU) 2.10

Which again will be used with three different Trilateration Algorithms

1. Matrix Product 2.12
2. Determinants 2.13. 2.14
3. System of Equations 2.15

Additionally, the number of devices that have Bluetooth enabled in public has been investigated.

Chapter 3

Research Method

This chapter will present what tools were used and how they were implemented. This is based on what the datasets needed to contain in order to evaluate the algorithms. Additionally, the research methodology that is followed throughout the thesis will also be presented.

3.1 Hardware and Software

The various hardware and software that has been utilized in the project will be clarified in this section. BLE beacons were used as transmitters during the measurements. Cellular phones, along with two different apps, were used as receivers, in addition to an On-board Unit (OBU).

3.1.1 Cellular Phones

Four different cellular phones have been used throughout the experiments. These are listed in table 3.1. The cellular phones have been utilized to measure and record BLE signals for different scenarios.

Cellular Phone	Samsung S21	iPhone 12	iPhone 13 ProMax	iPhone 15 ProMax
Chipset	Exynos 2100	A14 Bionic	A15 Bionic	A17 Pro
Bluetooth	5.0	5.0	5.0	5.3
OS while testing	Android 14	iOS 17.3.1	iOS 17.3.1	iOS 17.3.1
Release date	Jan 2021	Oct 2020	Sep 2021	Sep 2023
Specifications	[36]	[37]	[38]	[39]

Table 3.1: Cellular phones used in the thesis.

3.1.2 Beacons

The choice of beacons was partly based on the fact that UiS already had beacons in their possession, but also due to their specifications. Influenced by the thesis written by previous students at UiS, the iBKS105 was deemed suitable for the performance evaluation of algorithms [40], [41]. The beacons support both iBeacon and Eddystone, and with the iBKS Config Tool app, both the advertisement interval and the transmitting power level could be adjusted [42]. A low advertisement interval will provide a higher number of position estimations each second, which is important for tracking moving objects.

3.1.3 OBU

An OBU has several antennas installed, each configured to capture different signals. With the use of an OBU, the same wireless parameters that modern vehicles often come equipped with, becomes accessible. Modern vehicles tend to encapsulate this data into their manufacturers proprietary ecosystem, becoming inaccessible for private use.

The MK6 OBU from Cohda Wireless is equipped with Bluetooth 5.1, C-V2X, GNSS, Wi-Fi and more [43]. For this thesis, the parameters that were focused on are GNSS, Bluetooth and CANbus readings from the OBU. The MK6 OBU operates on Linux. To capture data, a Python script was used, developed in advance by Aitor, and used in this thesis [44].

3.1.4 GitHub CoPilot

As the use of AI continues to rise, commonly used by Computer Science students, was installed in the source-code editor of all the authors of this thesis [45]. Both to learn more about the tool itself, but also to increase efficiency while developing the code base.

3.1.5 Algorithm Modifications

The Determinant algorithm, eq. (2.14), did not function as intended when implemented the way suggested by [16]. It would find the correct x-value for a given set of distances and beacon positions, but the calculation for the y-value was incorrect. It would be equal to that of the x-value, but with the opposite sign. The plot generated by these coordinates resulted in a linear stream of points. Instead of continuing with this, a modification to the algorithm has been made. The new calculation for the y-value is proposed to be the following:

$$y = \frac{\begin{vmatrix} r_a^2 - r_b^2 - y_a^2 - y_b^2 - x_a^2 - x_b^2 & 2(x_b - x_a) \\ r_a^2 - r_c^2 - y_a^2 - y_c^2 - x_a^2 - x_c^2 & 2(x_c - x_a) \end{vmatrix}}{\begin{vmatrix} 2(y_b - y_a) & 2(x_b - x_a) \\ 2(y_c - y_a) & 2(x_c - x_a) \end{vmatrix}} \tag{3.1}$$

3.1.6 EFR Connect App

When starting this thesis, the availability of BLE detection tools was limited, but the EFR Connect app was available on both the App Store and Google Play Store [46]. This app has been used as a measuring and recording tool for various experiments in the thesis, but with caution, as its source code is not available to the public.

3.1.7 BLE Scanner App

A mobile app was developed using the Flutter framework to address the shortcomings of current market applications and to support data capture during measurements [47]. Inspiration for the structure of the app was the source code from, which was then further developed [48]. The basic functionalities that were developed and improved include: scanning for nearby devices, capturing the data, saving the data to CSV for analysis. The captured data would be used to represent the static scenario of pedestrians.

```
1 // BLE Controller Functionalities
2 CLASS BleController
3     // Check permissions before scanning
4     FUNCTION scanDevices
5         CHECK Bluetooth and Location Permissions
6         IF Permissions Granted THEN
7             Start Scanning
8         ELSE
9             Handle Permission Errors
10
11  // Start BLE Scanning Process
12     FUNCTION startScan
13         Clear previous data
14         Set scanning state to true
15         Subscribe to scan results
16         Stop scan on timeout or manually
17
18     // Stop Scanning
19     FUNCTION stopScan
20         Unsubscribe from scan
21         Set scanning state to false
22
23     FUNCTION saveCsvFile
24         Save CSV file using device storage access framework
```

Code 3.1: Pseudo-code for the BLE-controller part of the mobile app. The controller handles all operations related to BLE scanning.

The controller in 3.1 handles all the operations that are executed before, during and after a scan. The user is able to start and stop a scan through the GUI, as well as exporting files as seen in 3.1 line 26. All these functions allow for a functioning BLE-scanning app that serves as a tool for this thesis.

```
// Main App Initialization
    Initialize Application
    Initialize Controller

// User Interface Components
CLASS HomePage
    Handle Scan Control and Display Scan Results

    // Scan Control Widget
    CLASS ScanControlWidget
        Display and manage settings

    // Device List Display
    CLASS DeviceList
        List detected devices and show details
```

Code 3.2: Pseudo-code for the home page of the mobile app, demonstrating the initialization and user interface components.

The home page of the mobile app, as shown in figure 3.1a, utilizes the flutter framework to build widgets that are able to display the scan results in real-time as seen in Figure 3.1b.

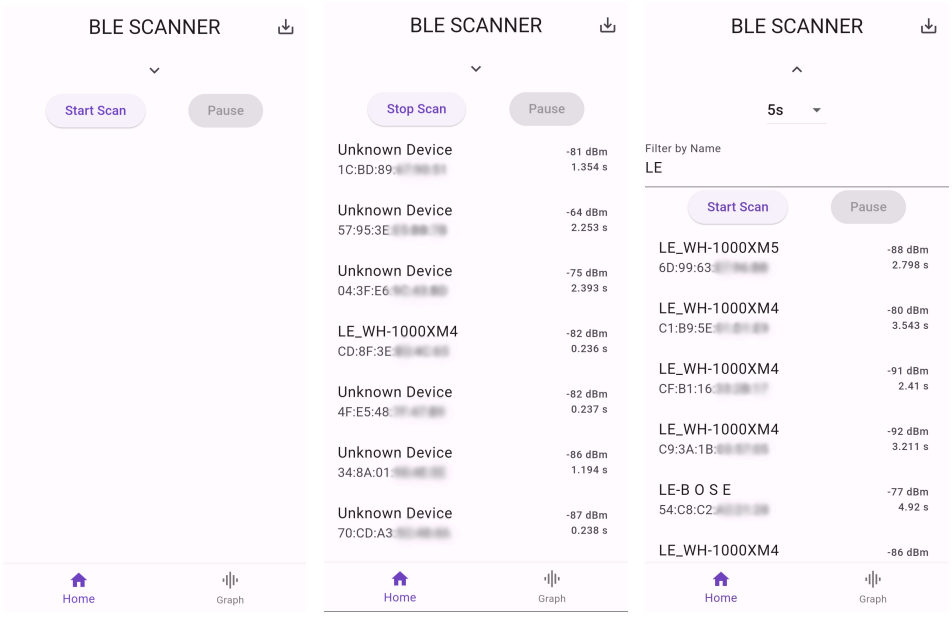

(a) Homepage of the app **(b)** A live scan **(c)** Dropdown menu

Figure 3.1: Full overview of the app with a start scan button, export button (top right), and a dropdown menu. The dropdown menu expands and allows users to set a duration for the scan as well as filtering results by name. Full device addresses are anonymized to comply with privacy standards.

3.2 Experimental Approach With Measurements

Tools that allow for data capture were used to assist in the experimental approach that is followed in the thesis. The experimental approach involves measurements taken in environments such as public bus rides, as well as static and dynamic scenarios inside of tunnels.

3.2.1 Experimental Approach: Public Bus Rides

The goal with these experiments was to collect datasets that could make a correlation on how many cellular devices were found on a bus, and then compare it to how many people that were on said bus ride. With this, it could be argued that a given amount of people will leave Bluetooth on in public areas, making a BLE approach for an IPS a valid solution. These datasets were captured with the EFR Connect app.

3.2.2 Experimental Approach: In-tunnel measurements

Due to the lack of research and data of how BLE Beacons perform inside tunnels, it was deemed necessary to conduct measurements. The measurements would provide insight into how transmitted signals from the BLE Beacons behave in the two main use cases, which are static and dynamic. Thus it was necessary to capture the transmitted signals both statically and dynamically, with the use of the tools that have been mentioned previously. The BLE Scanner App, clarified in section 3.1.7, was used to capture signals for the static scenarios. Additionally, the OBU, addressed in 3.1.3, was used to capture signals for the dynamic scenarios.

Chapter 4

Experimental Setup

The experimental approach in this thesis was split into two parts. The first part was to see how many people would have Bluetooth enabled on their cellular phones during a bus ride, from one stop to another. The second part was to see how different positioning algorithms performed in a tunnel. This chapter will present the setup for both of these scenarios.

4.1 Bus measurements

With the use of the EFR Connect app and cellular phones, datasets could be collected onboard public transport. These datasets were collected from a given bus stop, until the next one. This would ensure that no passengers would leave the bus in transit, and while in transit, the amount of people onboard was counted (including the driver) and noted. The majority of these datasets were collected on the same route, from stop **Gauselvågen** until **Rogaland Rideklubb**. The same approach was used for the other trips where BLE measurements were recorded, and the data was collected for the entire duration of all bus rides.

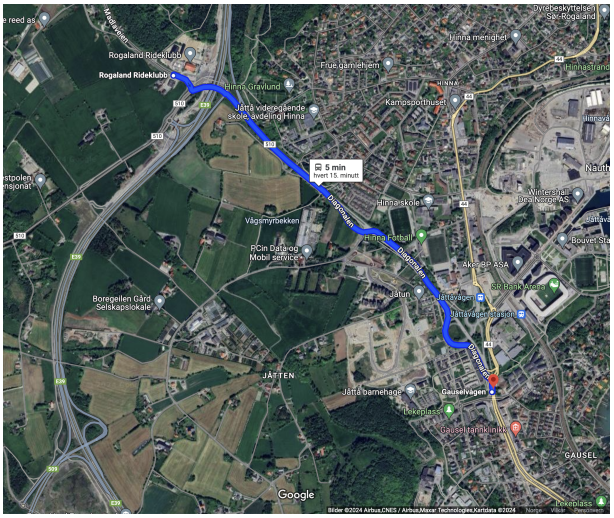

Figure 4.1: The route used to collect most datasets. The total distance is 2.1km and duration without traffic is 3 minutes, and 5 minutes with traffic. Picture from Google Maps [49].

4.2 In-tunnel measurements

The experimental approach for the in-tunnel measurements is designed to capture signals from nearby BLE Beacons, and then analyze the captured data. The BLE Beacons must be evenly spaced throughout the tunnel, as seen in Figure 4.2, and they must emit their signals with a low advertisement interval.

For the in-tunnel measurements the BLE beacons were configured to send an advertisement packet ten times per second, as well as increased Tx power to maximize the signal range. The RSSI of the signal from the incoming advertisement packet was then measured by the receiving device. Increasing the parameters of the configuration comes at a cost of battery life, depending on the intended use case the parameters could be decreased to lower maintenance costs.

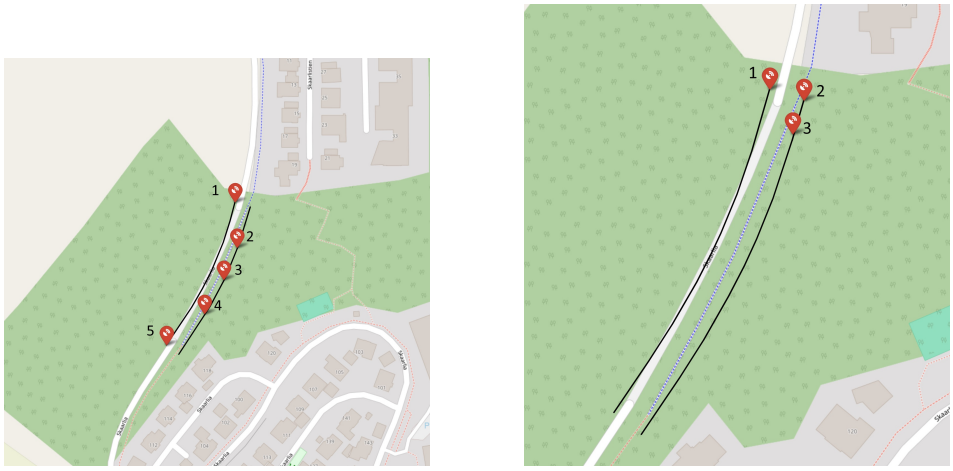

(a) Primary Beacon Placement. **(b)** Alternative Beacon Placement.

Figure 4.2: Various beacon placements for all of the experiments that were ran in the Skaarlia tunnel. The Skaarlia tunnel is located in Skaarlia, Sandnes Kommune, 4326 Norway. Each map is created with the Folium package in Python, which is built upon the OpenStreetMap database [50].

In total, five BLE beacons were used. These were attached to the tunnel wall with duct tape and placed at shoulder height, roughly 1.5m above the ground. The tunnel is 103m long, and the five beacons were evenly distributed along its total length. This beacon setup is called the primary setup.

The primary beacon setup, used for both the static and dynamic measurements, the beacons where placed 0, 25, 50, 75 and 100m into the Skaarlia tunnel. These placements correlate to the positions 1, 2, 3, 4 and 5 marked in Figure 4.2a. With the increase in Tx power, this setup allowed a receiver to always capture signals from at least three beacons.

Additionally, an alternative setup was tested for the static measurements. With three beacons placed in positions 1, 2 and 3, marked in Figure 4.2b. This setup was designed to see the impact of beacon placement for the algorithms. This setup spaced the beacons approximately 11m apart, with the goal of determining the optimal beacon placement for the algorithms. Table 4.1 contains all details for the two beacon setups.

Parameter \ Setup	Primary Setup	Alternative Setup
Number of Beacons	5	3
Beacon Height	1.5m	1.5m
Tx Power	+4dBm	+4dBm
Advertisement interval	100ms	100ms
Beacon Placement	4.2a	4.2b

Table 4.1: An overview of the configuration of the two beacon setups.

To provide a basis for comparison between static and dynamic use cases, the in-tunnel measurements are structured as follows:

- Static measurements were taken with discrete increments, with each increment being 1m. From 0-103m, giving 103 measurement sets in total. The primary setup was used, as seen in figure 4.2a.
- Static measurements were taken with discrete increments, with each increment being 1m. From 0-11m, giving 12 measurements in total. The alternative setup was used, as seen in figure 4.2b.
- Dynamic measurements were done in 5 round trips through the tunnel. The primary setup was used, as seen in figure 4.2a.

To capture these datasets during the measurements, two different tools were used. For the static measurements, the receiver of the signals was a handheld device, utilizing the app designed in section 3.1.7 to capture nearby signals. For the dynamic measurements, a Ford Mondeo 2009 with an installed OBU was used to capture various signals as it drove through the tunnel. The OBU captured BLE signals, GNSS signals available during the measurements, and CANbus data from the car. Throughout all dynamic measurements, the car maintained an average speed of 50 km/h. The datasets from the measurements are then defined as a collection of RSSI values from nearby BLE devices.

(a) Tunnel entrance, at the bottom of the hill in Skaarlia.

(b) GNSS antenna placed on the roof of the car.

(c) OBU mounted in the car. Powered by the car with an OBD2 connector.

Figure 4.3: Pictures taken during the day of the in-tunnel measurements.

Figure 4.3a depicts the tunnel entrance, with the left side of the arch, correlating to position 2 marked in Figure 4.2b, and the right hand side of the arch correlating to marked position 1.

The OBU was installed in the Ford Mondeo in such a way that the antennas had the least amount of blockage in front of them. To ensure clear LoS from the window, the OBU was mounted on the dashboard as shown in Figure 4.3c. It was powered from the car using a self-made OBD2 connector.

Chapter 5

Experimental Results

The results obtained from the tunnel-experiments generated coordinates that were heavily dependent on the placement of the beacons. The primary setup proved to be performing worse than the alternative setup for all scenarios.

Each of the three trilateration algorithms that were evaluated, provided identical coordinate estimations for any given set of distances and beacon locations.

Consequently, all three trilateration algorithms will be considered as one, and the performances of RSSI filters in combination with different distance estimations will be provided.

5.1 Static Measurement Results

The primary beacon setup had high average positioning errors, as depicted in Figure 5.1. As seen in Table 5.1, the lowest average error comes from the combination of SDOR & E at 84.43m. The lowest standard deviation comes from SMA & E, at 14.52m, and the lowest 90th percentile comes from SDOR & E at 105.74m.

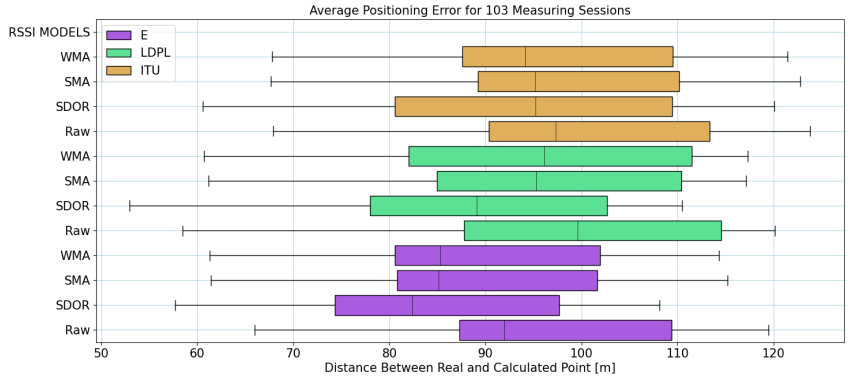

Figure 5.1: The distances between the 103 measured points and the real points were evaluated for all 12 combinations of an RSSI filter and a distance estimation algorithm in the primary setup. The y-axis depicts the RSSI model used, while each color represents a distance estimation algorithm.

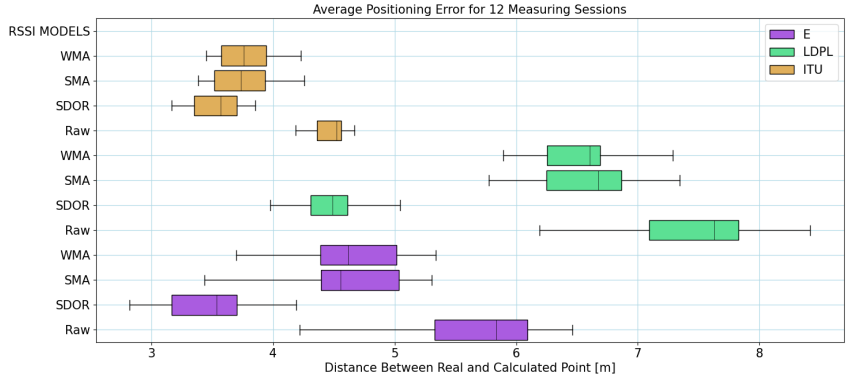

Figure 5.2: The distances between the 12 measured points and the real points was evaluated for all 12 combinations of an RSSI filter and a distance estimation algorithm in the alternative setup. The y-axis depicts the RSSI model used, while each color represents a distance estimation algorithm.

Combinations	Primary Setup			Alternative Setup		
	Avg	SD	90th%	Avg	SD	90th%
WMA & E	88.68	14.84	110.65	4.6	0.58	5.25
SMA & E	89.02	14.52	111.07	4.58	0.58	5.26
SDOR & E	84.43	14.86	105.74	3.48	0.39	3.96
Raw & E	95.14	15.28	117.41	5.63	0.62	6.14
WMA & LDPL	94.74	17.42	115.0	6.34	0.73	6.96
SMA & LDPL	94.7	16.42	114.51	6.42	0.79	7.16
SDOR & LDPL	87.85	16.61	118.89	4.49	0.31	4.9
Raw & LDPL	98.63	16.88	107.24	7.31	0.88	7.91
WMA & ITU	96.04	16.19	118.49	3.78	0.26	4.13
SMA & ITU	97.22	15.94	119.79	3.75	0.28	7.16
SDOR & ITU	94.31	17.96	117.36	3.57	0.33	3.84
Raw & ITU	99.17	16.19	121.78	4.47	0.15	4.62

Table 5.1: Numerical values of the performances of the Primary Setup and the Alternative Setup given in meters. The table displays the average, standard deviation and the 90th percentile values for the different algorithm combinations. Parameters used: $\gamma = 2.0$, $A =$ -58, $SD_c = 2$, $RSSI_0 =$ -12. $n = 10$.

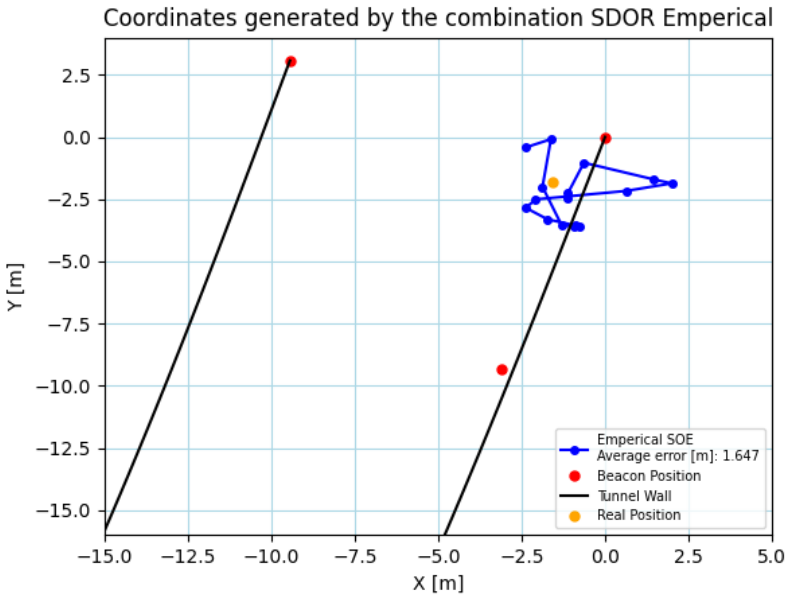

Figure 5.3: The results generated by a single measuring session for the alternative beacon setup. This single run had a low average error.

The alternative beacon setup had lower average positioning errors. As seen in Table 5.1, the lowest average error comes from the combination of SDOR & E at 3.48m. The lowest standard deviation comes from raw RSSI signals & ITU, at 0.15m, and the lowest 90th percentile comes from SDOR & E at 3.96m.

5.2 Dynamic Measurement Results

For the dynamic results, only the primary beacon setup was tested. Figure 5.4 depicts the inaccuracy of the performance of each algorithm combination for the dynamic scenario.

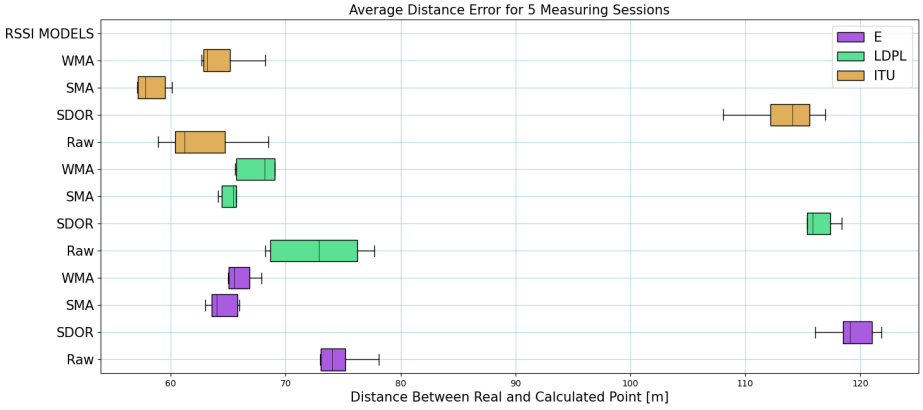

Figure 5.4: Dynamic measurements accuracy graph, represented in average distance error for the measuring sessions.

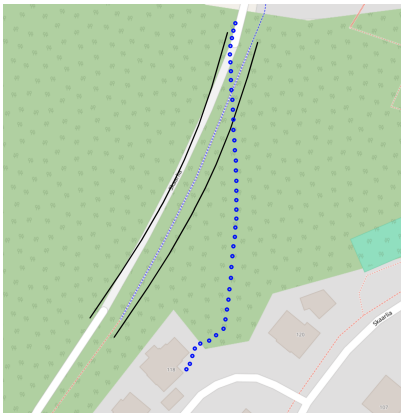

(a) GNSS from one dynamic measurement plotted on a map. The blue dots are the Lat/Lon coordinates, and the black lines are the estimated tunnel walls. Created using the OpenStreetMap database [50].

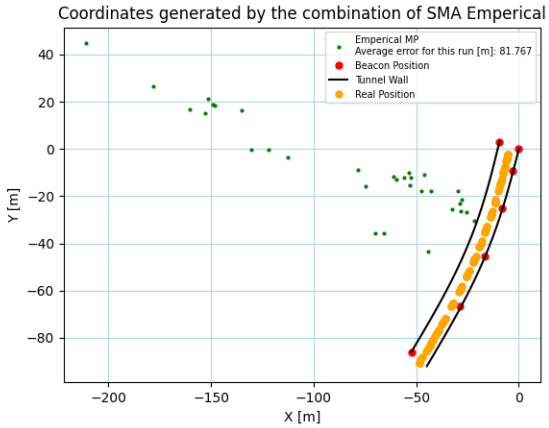

(b) Coordinates generated by SMA & Emperical while driving up through the tunnel.

Figure 5.5: GNSS and BLE coordinates generated from one run, up through the tunnel.

Combinations	Primary Setup		
	Avg	SD	90th%
WMA & E	66.06	1.29	67.5
SMA & E	64.45	1.35	65.89
SDOR & E	119.3	2.27	121.52
Raw & E	74.69	2.11	76.94
WMA & LDPL	69.39	5.28	74.67
SMA & LDPL	67.27	5.31	72.29
SDOR & LDPL	115.18	3.74	118.01
Raw & LDPL	72.74	4.29	77.11
WMA & ITU	64.42	2.35	67.0
SMA & ITU	58.33	1.38	59.85
SDOR & ITU	113.39	3.45	116.4
Raw & ITU	62.74	3.87	66.99

Table 5.2: Numerical values of the performance of the Primary Setup for the Dynamic measurements given in meters. The table displays the average, standard deviation and the 90th percentile values for the different algorithm combinations. Parameters used: $\gamma = 2.3$, $A =$ -58, $SD_c = 2$, $RSSI_0 =$ -12. $n = 3$.

As seen in Table 5.2, the lowest average error comes from the combination of SMA & ITU at 58.33m. The lowest standard deviation comes from WMA & E, at 1.29m, and the lowest 90th percentile comes from SMA & ITU at 59.85m.

Measurement Number	Mean Distance	Std. Deviation	90th Percentile
1	19.45	11.51	35.11
2	9.49	2.57	11.77
3	7.98	3.02	10.84
4	11.03	3.69	14.93
5	7.77	2.99	12.61
Total	11.13	4,76	17.05

Table 5.3: Statistical Analysis of GNSS Data from Dynamic Measurements, given in meters.

Figure 5.5a plots the GNSS location of the vehicle during one measurement. The inaccuracy is accumulated rapidly right after entering the tunnel, with estimated mean error for that measurement being 19.45 meters as seen in Table 5.3. The table also show that the accuracy is not consistent, as seen from the overall standard deviation, on average deviating 6.27 meters from the mean distance. Some of the 90th percentile values are high for individual measurements, but overall they fall under 19.49 meters.

As for the CANbus data retrieved from the car, the data is difficult to make sense of. The CAN IDs are Ford proprietary, and they are not disclosed publicly. As a result, the data was rendered fruitless for the use in this thesis.

5.3 Bus Measurement Results

While analyzing and visualizing the data, a large amount of MAC/UUID addresses had their peripheral name labeled as "N/A". Therefore, the results of these experiments are divided into two parts: One with data where devices named "N/A" are present, and the other where they are not.

Date	People	Address with "N/A"	Address without "N/A"	Named address %
07/02/24	23	315 (60)	58 (14)	18.4% (23.3%)
09/02/24	14	285 (41)	46 (8)	16.1% (19.5%)
10/02/24	15	383 (125)	76 (30)	19.8% (20%)
13/02/24	20	272 (41)	53 (6)	19.5% (14.6%)
14/02/24	21	736 (116)	87 (15)	11.8% (12.9%)
21/02/24	13	988 (138)	91 (24)	9.2% (17.4%)
23/02/24	8	133 (56)	19 (5)	14.3% (8.9%)
28/02/24	15	332 (50)	46 (6)	13.9% (12%)
29/02/24	10	338 (104)	50 (20)	14.8% (19.2%)
01/03/24	9	228 (71)	26 (13)	11.4% (18.3%)
06/03/24	23	425 (104)	55 (14)	12.9% (13.5%)

Table 5.4: An overview of the number of people on the bus, unique addresses detected including those that are named "N/A", and when the "N/A" are filtered out, a comparison in percentage. The numbers in parentheses are devices that were not persistent for the whole duration.

Unique addresses that did not persist for the whole duration, were filtered out and counted separately. These are devices that likely have been picked up while driving, e.g. pedestrians or cars in traffic, but they are still counted and shown in Table 5.4.

The results show a large difference in the amount of unique addresses detected when the devices named "N/A" are included, compared to when they are not, as shown in Table 5.4. In Figure 5.6a, the 10th and 90th percentiles for the RSSI values depicts that the majority of devices are in close proximity. This is also true when including unique addresses that are named "N/A" as shown in Figure 5.6b.

The percentage of devices that are persistent, compared to those that are

not, do not vary much as seen in 5.4. When the devices names "N/A" are included, the total number of unique addresses is more than seven times higher than when they are omitted.

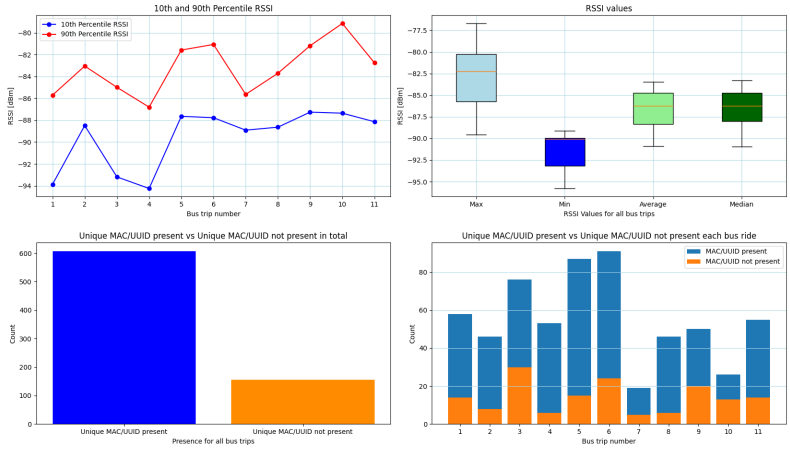

(a) Data from bus rides without MAC/UUID addresses named "N/A".

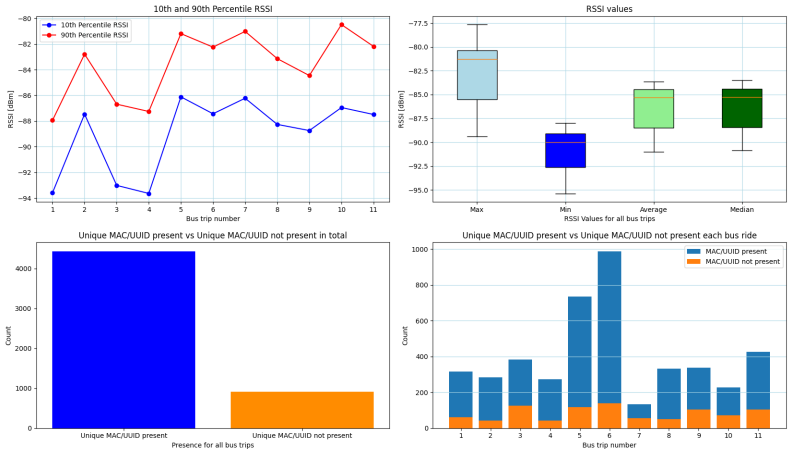

(b) Data from bus rides with MAC/UUID addresses named "N/A".

Figure 5.6: Comparison of data from bus rides with and without MAC/UUID addresses named "N/A".

Chapter 6

Discussion

This chapter is dedicated to the discussion of the results from the previous chapters. The results will be compared to the GNSS, and a reasoning for the inaccuracies will be provided. As the performance of the algorithms depended more on the beacon's position, rather than if the scenario was dynamic or static, the chapter will be split into three sections: Primary Setup Discussion, Alternative Setup Discussion and Bus Measurement Discussion.

6.1 Discussion: Primary Setup

From the primary setup in Figure 5.1 it can be argued that the combination of WMA and LDPL is not the only combination that is performing poorly. Although it was stated to be the worst performing, most of the algorithms are in fact performing similar. However, this combination is definitely the most unreliable, with a standard deviation of 17.42, the highest amongst them all, and 90% of the values fall below 115.0 as seen in Table 5.1. All of the distances calculated with any form of LDPL combination, result in high variance. This could be due to the random shadowing effect parameter, or because of a poor choice of path loss exponent. The LDPL and Empirical model share the same path loss exponent in their calculations, and they both genereally perform worse than ITU, as seen in Figure 5.4.

When comparing the dynamic measurement results of the algorithms to the GNSS signals it is clear that the GNSS yield better results. GNSS had an average error of 11.13 meters, while SMA & ITU, the best performing combination of algorithms for the dynamic scenario, had an average of 58.33 meters.

The dynamic measurements achieved better results than the static measurements in terms of average error, standard deviation and 90th percentile. This is in contradiction to the expected behaviour, as the static measurements were captured from one location for a longer period of time. Because the primary beacon setup performed so poorly in both scenarios, the positioning of the beacons will be explored in depth.

The irregular behavior seen in Figure 5.4 and Figure 5.2 stems from three main factors. Beacons in position 2, 3 and 4, mentioned in Figure 4.2a, are near collinear. This results in a poor performance for the trilateration algorithms. This is further enhanced by the way the distance estimation algorithms converts RSSI to meter at lower RSSI values. Additionally, a parameter analysis will be provided to display the sensitivity of the path loss exponent.

6.1.1 Beacon Placement Analysis

To illustrate the problem of beacon placement, an analysis of the algorithms was performed. Figure 6.1 displays the behaviour of all trilateration algorithms, as the three beacons become increasingly collinear.

If the distance estimations are perfectly accurate, the placement of the beacons are irrelevant, as seen from the blue graph in Figure 6.1. As the distance estimations deviate from their perfect values, however, errors for the positioning algorithms can be observed. As seen in both the green and orange graphs in Figure 6.1, this deviation is exponentially enhanced as B2 is shifted towards B1. When there is only 1 meter between B1 and B2 in the x-axis, the positioning error increases to approximately 175m for the case where B1 and B3 have been given distances that are 8 meters lower than the perfect value, visualized in the green graph.

Therefore, it can be determined that inaccuracies in the distance estima-

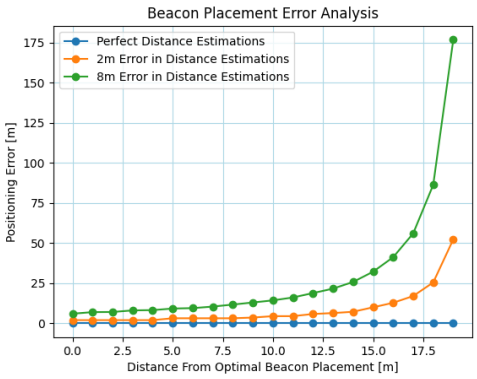

(a) Performance of beacon displacement.

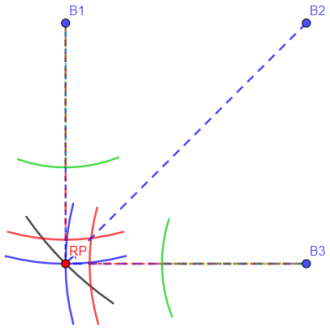

(b) Beacon setup used in the analysis.

Figure 6.1: Performance analysis of the trilateration algorithms for when Beacon 2 (B2) in figure **(b)** was shifted along the x-axis, towards Beacon 1 (B1). The color of the circular arcs represents the three different radii used in the analysis. The radius from B2 to the Real Point (RP) was the only distance which was always set to the correct length.

tions contribute to the inaccuracies in the positioning algorithms. These inaccuracies are exponentially enhanced by poor beacon placements.

6.1.2 Distance Estimations at Low RSSI

As poor distance estimations negatively affects the final position estimation, having a reliable distance estimation algorithm is crucial. Figure 6.2 depicts the real, measured RSSI at the distances 1, 2, ..., 49, 50m away from a beacon inside of the tunnel. Additionally, the three distance estimation models have been added as well.

When the distance between the receiver and the transmitter is below 10 meters, the accuracy of the distance estimation algorithms are higher. At longer distances, however, when the curves flattens out, the impact that a single shift in dBm has on the distance estimation algorithm increases. For instance the Emperical Model converts the RSSI value -81 dBm to 42.8 meters, while an RSSI value of -82 dBm converts to 48.3 meters, a difference of 5.5 meters. And as mentioned in section 6.1.1, a 5.5 meter error in the distance estimation can lead to an even larger inaccuracy for the position

estimation.

Considering this, it can be explained why the estimated positions presented for the dynamic measurements had a high degree of error. When looking at the real point (-32, -65), approximately at the center of the tunnel, the real distances from the point to the three closest beacons are 4, 25 and 28 meters. The estimated distances, however, were calculated to be 3, 16 and 25 meters. The estimated position then becomes (54, -133), which is 216 meters away from the real point.

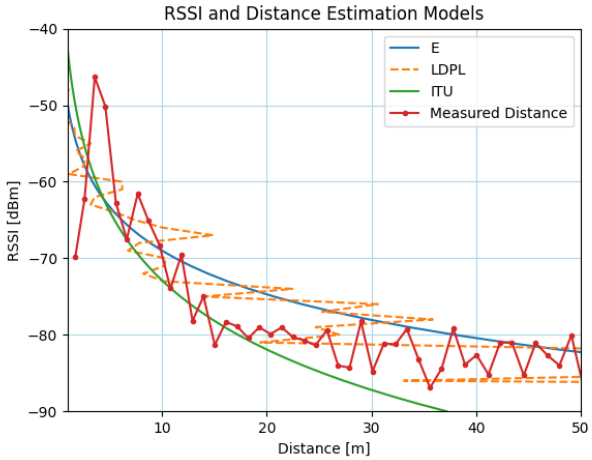

Figure 6.2: Captured RSSI at certain, measured distances away from a beacon, plotted against the calculated result from the distance estimation algorithms. The distance estimation algorithms used the parameters $\gamma = 1.9$, and the Rx level $A = -50$.

6.1.3 Parameter Analysis

The value of the path loss exponent, γ, drastically impacted the accuracy of the calculated coordinates. The calculated value of γ was found to be 2.11 at the tunnel arch 2.5. At 25 meters into the tunnel however, the calculated γ changed to 2.6. 50 meters into the tunnel, it changed again to 1.6.

As shown in figure 6.3a, the overall best performing γ value is 2.3. When

looking at a single run, however, it becomes evident that the optimal γ value changes as the car moves through the tunnel. As seen in 6.3b, the best performing γ fluctuates between the plotted values. At the start of the tunnel, the best γ value is 1.9, then the best value increases to 2.1, then to 2.3, and so on.

It can therefore be presumed that a dynamic value for γ will increase the accuracy for all the distance estimation algorithms in a tunnel environment.

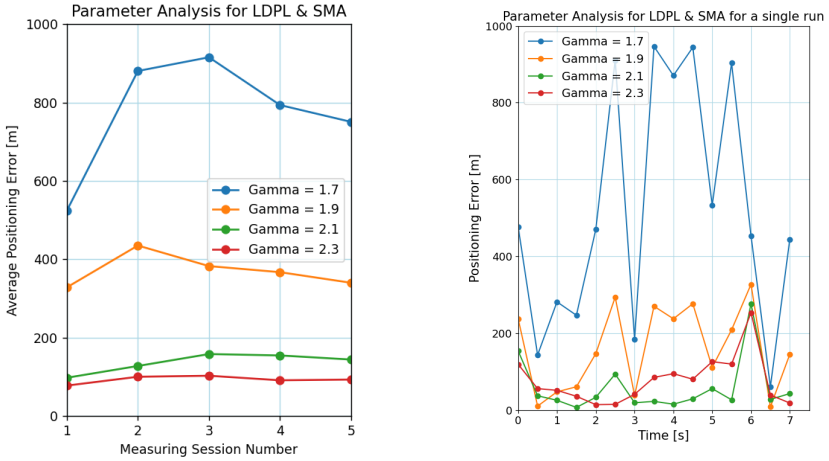

(a) Data taken from the average of 5 runs. **(b)** Data taken from a single run.

Figure 6.3: The impact different γ values has on the performance of the trilateration algorithms.

6.2 Alternative Beacon Setup

The alternative beacon setup is more representative of the performance of the different algorithm combinations. The results from the alternative setup produced usable results, unlike that of the primary setup.

The ITU model is complex due to its specific parameters, designed to address the various aspects of indoor signal propagation, and this is reflected in the results. The ITU model performs the best overall, as it has low average errors and standard deviations with all filters. This is likely due to the

fact that the value for γ, which the two other distance estimation use, was set to be a constant number. This produced poor results, as mentioned in subsection 6.1.3, as the optimal value for γ changes throughout the tunnel.

The SDOR is the best performing RSSI filter. When this filter is applied to any of the distance estimation algorithm, it increases the accuracy more than any of the other filters. This is because it is designed to filter out the lowest values received, as opposed to the other two filters. Both SMA and WMA treats these low values as if they were normal ones. As the results show, removing these low values increase the performance.

The best performing combination of algorithm is the Empirical model along with the SDOR filter. Even though the ITU model was better overall, the Empirical model produced the very best results with the SDOR filter. This implementation had an average error of 3.48 meters, which likely can be lowered further with the implementation of a dynamic path loss exponent.

6.3 Bus Measurement Discussion

During the analysis of the data collected from the bus measurements, it was observed that a significant number of devices with the name "N/A" were present. This could be due to the BLE Privacy feature which protects devices against BLE scanning. This feature causes the MAC address in the advertising packets to be replaced by a random value that changes at intervals determined by the manufacturer [32]. As a result, advertisement packets from devices with BLE privacy enabled will keep changing their MAC addresses. Consequently, it becomes difficult to determine the number of devices on the bus, as there are no way to determine the frequency of these randomizations for each individual device.

Devices that are named in clear text constitutes roughly 9-20% of all the devices that are found when scanning for devices with the EFR Connect app, as shown in Table 5.4. When looking at device names, they are often correlated with devices that are IoT devices, headsets, smart watches or other accessories. The name of a cellular phone in clear text was never found in the data.

6.3 Bus Measurement Discussion

The data that has been presented shows no correlation between the number of people present on the bus, and the number of devices found with the EFR Connect app. MAC addresse randomization plays a large factor to this.

To de-randomize the Bluetooth MAC addresses, in an uncontrolled environment with a large set of devices, is described as nearly impossible [51].

In controlled areas, experiments were conducted to find cellular phones using the EFR connect app. While there were readings of RSSI values that corresponded to the distances, a corresponding device name or MAC addresse could not be found. It is reasonable to assume that most of the devices named "N/A" are mobile devices that have their MAC addresses randomized.

Chapter 7

Conclusion

The algorithms that have been evaluated in the thesis **are not superior** to GNSS in a short tunnel. The inaccuracy of the dynamic implementation was immense, and the results were not usable for a real IPS implementation. The poor results can be attributed to the placement of the beacons, the large distance between them and the use of a static path loss exponent during the analysis.

Answers to the the three research questions that were raised have been found.

7.1 Research Question 1

Firstly, which algorithm had the highest accuracy in a dynamic scenario? As shown in Figure 5.4 the ITU model is the best performing distance estimation algorithm. The SMA filter is the best performing filter, and for all distance estimation algorithms, the results with the SMA filter applied are superior to the others. The best performing combination was found to be the combination of ITU and SMA.

7.2 Research Question 2

Secondly, which algorithm has the highest accuracy in a static scenario? For the primary beacon setup in the static scenario, the Empirical distance estimation model had the best performance as seen in Figure 5.1. The SDOR filter improved the accuracy of all distance estimations algorithms, and the best performing combination, was the combination of SDOR and Empirical. For the alternative beacon setup the ITU model was, again, the superior distance estimation model overall, and the SDOR filter was the best performing filter for all distance estimation algorithms. However, the best performing combination proved to be SDOR and Empirical for the alternative beacon setup for the static scenario. This means that under ideal conditions where the alternative setup is possible, i.e, in smaller tunnels meant for pedestrians only, the IPS could rely on SDOR filtering and the Empirical model.

7.3 Research Question 3

Finally, will this approach improve accuracy over current solutions? When comparing dynamic results from Table 5.2, with the GNSS results from Table 5.3, the accuracy from the dynamic results are worse than GNSS. With the primary beacon setup, the algorithms that have been tested do not perform well for a moving vehicle. As the GNSS had an average error of 11.13m, while the dynamic results had the lowest average error at 58.33 meters. Even when GNSS signals fade, the current solutions is still more accurate for a dynamic scenario than the proposed approach.

In a static scenario using the alternative beacon setup, the lowest average error was 3.48 meters. This level of accuracy could potentially allow emergency services to pinpoint the location of injured pedestrians or crashed vehicles. In situations with heavy smoke and a dangerous environment, a 3.48 meter error margin can prove to be useful.

7.4 Future Work

For future work on IPSs in tunnels, upgrading the hardware could lead to better results by enabling the measurement of AoA. Since related work shows promise for AoA's accuracy in IPSs in general, it could potentially improve the accuracy of BLE-based IPS in tunnels as well.

Additionally, experimenting with different beacon placements inside a controlled tunnel environment could positively affect the results. The proposed approach based on this thesis' results would be to form a sequence of squares of the BLE Beacons throughout the tunnel.

When experimenting with different beacon placements, it would also be worthwhile to explore the path loss exponent. A dynamic path loss exponent could produce better results for tunnel environments.

Bibliography

[1] A. Bruland, R. Hugsted, and R. S. Nordahl, *Tunnel*, no, Jan. 2024. [Online]. Available: https://snl.no/tunnel (visited on 05/07/2024).

[2] Statens vegvesen, *Statens vegvesen - Informasjon til brukerne av Ryfast*, Nov. 2019. [Online]. Available: https://www.youtube.com/watch?v=s_PzGmaQ0-M (visited on 05/07/2024).

[3] M. Brossard, A. Barrau, and S. Bonnabel, "AI-IMU Dead-Reckoning", *IEEE Transactions on Intelligent Vehicles*, vol. 5, no. 4, pp. 585–595, Dec. 2020, Conference Name: IEEE Transactions on Intelligent Vehicles, ISSN: 2379-8904. DOI: 10.1109/TIV.2020.2980758. [Online]. Available: https://ieeexplore.ieee.org/abstract/document/9035481 (visited on 05/08/2024).

[4] A. James, *How can IMUs improve AV positioning accuracy and operational safety?*, en-GB, Feb. 2021. [Online]. Available: https://www.autonomousvehicleinternational.com/features/how-can-imu-technology-improve-positioning-accuracy-and-operational-safety-for-avs.html (visited on 05/08/2024).

[5] D. Zaim and M. Bellafkih, "Bluetooth Low Energy (BLE) based geomarketing system", in *2016 11th International Conference on Intelligent Systems: Theories and Applications (SITA)*, ISSN: 2378-2536, Oct. 2016, pp. 1–6. DOI: 10.1109/SITA.2016.7772263. [Online]. Available: https://ieeexplore.ieee.org/abstract/document/7772263 (visited on 05/06/2024).

[6] L. Qi, Y. Liu, Y. Yu, L. Chen, and R. Chen, "Current Status and Future Trends of Meter-Level Indoor Positioning Technology: A Review", en, *Remote Sensing*, vol. 16, no. 2, p. 398, Jan. 2024, Number: 2 Publisher: Multidisciplinary Digital Publishing Institute, ISSN: 2072-

4292. DOI: 10.3390/rs16020398. [Online]. Available: https://www.mdpi.com/2072-4292/16/2/398 (visited on 05/07/2024).

[7] H. Ye, B. Yang, Z. Long, and C. Dai, "A Method of Indoor Positioning by Signal Fitting and PDDA Algorithm Using BLE AOA Device", en, *IEEE Sensors Journal*, vol. 22, no. 8, pp. 7877–7887, Apr. 2022, ISSN: 1530-437X, 1558-1748, 2379-9153. DOI: 10.1109/JSEN.2022.3141739. [Online]. Available: https://ieeexplore.ieee.org/document/9676583/ (visited on 01/25/2024).

[8] R. Bembenik and K. Falcman, "BLE Indoor Positioning System Using RSSI-based Trilateration", en, *Journal of Wireless Mobile Networks, Ubiquitous Computing, and Dependable Applications*, vol. 11, no. 3, pp. 50–69, Sep. 2020. DOI: 10.22667/JOWUA.2020.09.30.050. [Online]. Available: https://doi.org/10.22667/JOWUA.2020.09.30.050 (visited on 01/31/2024).

[9] M. Nabati and S. A. Ghorashi, "A real-time fingerprint-based indoor positioning using deep learning and preceding states", *Expert Systems with Applications*, vol. 213, p. 118 889, Mar. 2023, ISSN: 0957-4174. DOI: 10.1016/j.eswa.2022.118889. [Online]. Available: https://www.sciencedirect.com/science/article/pii/S0957417422019078 (visited on 05/08/2024).

[10] I. Ashraf, M. Kang, S. Hur, and Y. Park, "MINLOC:Magnetic Field Patterns-Based Indoor Localization Using Convolutional Neural Networks", *IEEE Access*, vol. 8, pp. 66 213–66 227, 2020, Conference Name: IEEE Access, ISSN: 2169-3536. DOI: 10.1109/ACCESS.2020.2985384. [Online]. Available: https://ieeexplore.ieee.org/abstract/document/9056514 (visited on 05/08/2024).

[11] M. Elsanhoury, P. Mäkelä, J. Koljonen, *et al.*, "Precision Positioning for Smart Logistics Using Ultra-Wideband Technology-Based Indoor Navigation: A Review", *IEEE Access*, vol. 10, pp. 44 413–44 445, 2022, Conference Name: IEEE Access, ISSN: 2169-3536. DOI: 10.1109/ACCESS.2022.3169267. [Online]. Available: https://ieeexplore.ieee.org/abstract/document/9761257 (visited on 05/08/2024).

[12] R. Yang, X. Yang, J. Wang, M. Zhou, Z. Tian, and L. Li, "Decimeter Level Indoor Localization Using WiFi Channel State Information", *IEEE Sensors Journal*, vol. 22, no. 6, pp. 4940–4950, Mar. 2022, Conference Name: IEEE Sensors Journal, ISSN: 1558-1748. DOI: 10.1109/JSEN.2021.3067144. [Online]. Available: https:

//ieeexplore.ieee.org/abstract/document/9381239 (visited on 05/08/2024).

[13] F. Qin, T. Zuo, and X. Wang, "CCpos: WiFi Fingerprint Indoor Positioning System Based on CDAE-CNN", en, *Sensors*, vol. 21, no. 4, p. 1114, Jan. 2021, Number: 4 Publisher: Multidisciplinary Digital Publishing Institute, ISSN: 1424-8220. DOI: 10.3390/s21041114. [Online]. Available: https://www.mdpi.com/1424-8220/21/4/1114 (visited on 05/08/2024).

[14] J. Brož, T. Tichý, R. Prokeš, A. Štencek, and T. Šmerda, "Proximity Approach to Bluetooth Low Energy-Based Localization in Tunnels", en, *Sustainability*, vol. 15, no. 4, p. 3659, Feb. 2023, ISSN: 2071-1050. DOI: 10.3390/su15043659. [Online]. Available: https://www.mdpi.com/2071-1050/15/4/3659 (visited on 01/17/2024).

[15] C. Asiminidis, G. Kokkonis, and S. Kontogiannis, "BLE Sniffing for Crowd Sensing and Directionality Scanning of Mobile Devices Inside Tunnels", en, in *2020 3rd World Symposium on Communication Engineering (WSCE)*, Thessaloniki, Greece: IEEE, Oct. 2020, pp. 54–58, ISBN: 978-1-72818-564-4. DOI: 10.1109/WSCE51339.2020.9275574. [Online]. Available: https://ieeexplore.ieee.org/document/9275574/ (visited on 01/17/2024).

[16] V. Cantón Paterna, A. Calveras Augé, J. Paradells Aspas, and M. A. Pérez Bullones, "A Bluetooth Low Energy Indoor Positioning System with Channel Diversity, Weighted Trilateration and Kalman Filtering", en, *Sensors*, vol. 17, no. 12, p. 2927, Dec. 2017, Number: 12 Publisher: Multidisciplinary Digital Publishing Institute, ISSN: 1424-8220. DOI: 10.3390/s17122927. [Online]. Available: https://www.mdpi.com/1424-8220/17/12/2927 (visited on 01/28/2024).

[17] F. Liu, J. Liu, Y. Yin, *et al.*, "Survey on WiFi-based indoor positioning techniques", en, *IET Communications*, vol. 14, no. 9, pp. 1372–1383, 2020, _eprint: https://onlinelibrary.wiley.com/doi/pdf/10.1049/iet-com.2019.1059, ISSN: 1751-8636. DOI: 10.1049/iet-com.2019.1059. [Online]. Available: https://onlinelibrary.wiley.com/doi/abs/10.1049/iet-com.2019.1059 (visited on 05/06/2024).

[18] A. Alarifi, A. Al-Salman, M. Alsaleh, *et al.*, "Ultra Wideband Indoor Positioning Technologies: Analysis and Recent Advances", en, *Sensors*, vol. 16, no. 5, p. 707, May 2016, Number: 5 Publisher: Multidisciplinary Digital Publishing Institute, ISSN: 1424-8220. DOI: 10.3390/

s16050707. [Online]. Available: https://www.mdpi.com/1424-8220/16/5/707 (visited on 05/06/2024).

[19] S.-C. Yeh, W.-H. Hsu, W.-Y. Lin, and Y.-F. Wu, "Study on an Indoor Positioning System Using Earth's Magnetic Field", *IEEE Transactions on Instrumentation and Measurement*, vol. 69, no. 3, pp. 865–872, Mar. 2020, Conference Name: IEEE Transactions on Instrumentation and Measurement, ISSN: 1557-9662. DOI: 10.1109/TIM.2019.2905750. [Online]. Available: https://ieeexplore.ieee.org/abstract/document/8683984 (visited on 05/06/2024).

[20] A. Morar, A. Moldoveanu, I. Mocanu, *et al.*, "A Comprehensive Survey of Indoor Localization Methods Based on Computer Vision", en, *Sensors*, vol. 20, no. 9, p. 2641, Jan. 2020, Number: 9 Publisher: Multidisciplinary Digital Publishing Institute, ISSN: 1424-8220. DOI: 10.3390/s20092641. [Online]. Available: https://www.mdpi.com/1424-8220/20/9/2641 (visited on 05/06/2024).

[21] G. M. Mendoza-Silva, J. Torres-Sospedra, and J. Huerta, "A Meta-Review of Indoor Positioning Systems", en, *Sensors*, vol. 19, no. 20, p. 4507, Jan. 2019, Number: 20 Publisher: Multidisciplinary Digital Publishing Institute, ISSN: 1424-8220. DOI: 10.3390/s19204507. [Online]. Available: https://www.mdpi.com/1424-8220/19/20/4507 (visited on 04/29/2024).

[22] Y. Yun, J. Lee, D. An, S. Kim, and Y. Kim, "Performance Comparison of Indoor Positioning Schemes Exploiting Wi-Fi APs and BLE Beacons", en, in *2018 5th NAFOSTED Conference on Information and Computer Science (NICS)*, Ho Chi Minh City: IEEE, Nov. 2018, pp. 124–127, ISBN: 978-1-5386-7983-8. DOI: 10.1109/NICS.2018.8606852. [Online]. Available: https://ieeexplore.ieee.org/document/8606852/ (visited on 03/20/2024).

[23] L. Klinkusoom, T. Sanpechuda, K. Maneerat, K. Chinda, and L.-O. Kovavisaruch, "Accuracy Comparison of Bluetooth Low Energy Indoor Positioning System based on measurement techniques", en, in *2022 IEEE International Conference on Consumer Electronics-Asia (ICCE-Asia)*, Yeosu, Korea, Republic of: IEEE, Oct. 2022, pp. 1–5, ISBN: 978-1-66546-434-5. DOI: 10.1109/ICCE-Asia57006.2022.9954806. [Online]. Available: https://ieeexplore.ieee.org/document/9954806/ (visited on 03/20/2024).

[24] S. Chai, R. An, and Z. Du, "An Indoor Positioning Algorithm using Bluetooth Low Energy RSSI", en, in *Proceedings of the 2016 International Conference on Advanced Materials Science and Environmental Engineering*, Chiang Mai, Thailand: Atlantis Press, 2016, ISBN: 978-94-6252-209-1. DOI: 10.2991/amsee-16.2016.72. [Online]. Available: http://www.atlantis-press.com/php/paper-details.php?id=25858154 (visited on 01/28/2024).

[25] S. Subedi, G.-R. Kwon, S. Shin, S.-s. Hwang, and J.-Y. Pyun, "Beacon based indoor positioning system using weighted centroid localization approach", in *2016 Eighth International Conference on Ubiquitous and Future Networks (ICUFN)*, ISSN: 2165-8536, Jul. 2016, pp. 1016–1019. DOI: 10.1109/ICUFN.2016.7536951. [Online]. Available: https://ieeexplore.ieee.org/document/7536951 (visited on 05/08/2024).

[26] S. Monfared, T.-H. Nguyen, L. Petrillo, P. De Doncker, and F. Horlin, "Experimental Demonstration of BLE Transmitter Positioning Based on AOA Estimation", en, in *2018 IEEE 29th Annual International Symposium on Personal, Indoor and Mobile Radio Communications (PIMRC)*, Bologna, Italy: IEEE, Sep. 2018, pp. 856–859, ISBN: 978-1-5386-6009-6. DOI: 10.1109/PIMRC.2018.8580796. [Online]. Available: https://ieeexplore.ieee.org/document/8580796/ (visited on 01/17/2024).

[27] C. S. Mouhammad, A. Allam, M. Abdel-Raouf, E. Shenouda, and M. Elsabrouty, "BLE Indoor Localization based on Improved RSSI and Trilateration", in *2019 7th International Japan-Africa Conference on Electronics, Communications, and Computations, (JAC-ECC)*, Dec. 2019, pp. 17–21. DOI: 10.1109/JAC-ECC48896.2019.9051304. [Online]. Available: https://ieeexplore.ieee.org/abstract/document/9051304 (visited on 01/28/2024).

[28] T. S. Rappaport, *Wireless communications: principles and practice* (Prentice Hall communications engineering and emerging technologies series), eng, 2. ed., 18. printing. Upper Saddle River, NJ: Prentice Hall, 2009, ISBN: 978-0-13-042232-3.

[29] N. Pakanon, M. Chamchoy, and P. Supanakoon, *Study on Accuracy of Trilateration Method for Indoor Positioning with BLE Beacons*, Dec. 2020. [Online]. Available: https://ieeexplore.ieee.org/stamp/stamp.jsp?tp=&arnumber=9165464 (visited on 01/17/2024).

[30] John, *Answer to "Find X location using 3 known (X,Y) location using trilateration"*, Aug. 2014. [Online]. Available: https://math.stackexchange.com/a/884851 (visited on 05/08/2024).

[31] A. Ozer and E. John, "Improving the Accuracy of Bluetooth Low Energy Indoor Positioning System Using Kalman Filtering", en, in *2016 International Conference on Computational Science and Computational Intelligence (CSCI)*, Las Vegas, NV, USA: IEEE, Dec. 2016, pp. 180–185, ISBN: 978-1-5090-5510-4. DOI: 10.1109/CSCI.2016.0041. [Online]. Available: http://ieeexplore.ieee.org/document/7881334/ (visited on 02/01/2024).

[32] M. Woolley, *Bluetooth TechnologyProtecting Your Privacy*, en-US, Apr. 2015. [Online]. Available: https://www.bluetooth.com/blog/bluetooth-technology-protecting-your-privacy/ (visited on 04/25/2024).

[33] S. Cortesi, C. Vogt, and M. Magno, "Comparison between an RSSI- and an MCPD-Based BLE Indoor Localization System †", English, *Computers*, vol. 12, no. 3, 2023, ISSN: 2073-431X. DOI: 10.3390/computers12030059.

[34] A. Blackstone, *Understanding the different types of BLE Beacons | Mbed*, Mar. 2015. [Online]. Available: https://os.mbed.com/blog/entry/BLE-Beacons-URIBeacon-AltBeacons-iBeacon/ (visited on 01/17/2024).

[35] M. Li, *What is Eddystone Beacon and how is Eddystone Beacon work?*, en-US, Aug. 2021. [Online]. Available: https://www.mokoblue.com/all-about-eddystone-beacon/ (visited on 04/25/2024).

[36] *Samsung Galaxy S21 5G - Full phone specifications*. [Online]. Available: https://www.gsmarena.com/samsung_galaxy_s21_5g-10626.php (visited on 04/28/2024).

[37] *Apple iPhone 12 - Full phone specifications*. [Online]. Available: https://www.gsmarena.com/apple_iphone_12-10509.php (visited on 04/28/2024).

[38] *Apple iPhone 13 Pro Max - Full phone specifications*. [Online]. Available: https://www.gsmarena.com/apple_iphone_13_pro_max-11089.php (visited on 04/28/2024).

[39] *Apple iPhone 15 Pro Max - Full phone specifications*. [Online]. Available: https://www.gsmarena.com/apple_iphone_15_pro_max-12548.php (visited on 04/28/2024).

[40] N. C. Grimstad, S. G. Kase, and S. F. W. Brandasu, "Innendørs Posisjoneringssystem for IDE ved bruk av Bluetooth Low-Energy Beacons", eng, Accepted: 2021-09-07T16:29:34Z, Bachelor thesis, uis, 2021. [Online]. Available: https://uis.brage.unit.no/uis-xmlui/handle/11250/2774387 (visited on 04/24/2024).

[41] Accent Systems, *iBKS105 Datasheet*, Jan. 2017. [Online]. Available: https://accent-systems.com/wp-content/uploads/iBKS105_datasheet_rev3.pdf (visited on 04/26/2024).

[42] *iBKS Config Tool*, en-GB, Apr. 2019. [Online]. Available: https://apps.apple.com/no/app/ibks-config-tool/id929525388 (visited on 04/28/2024).

[43] *MK6 OBU*. [Online]. Available: https://www.cohdawireless.com/wp-content/uploads/2022/09/CW_Product-Brief-sheet-MK6-OBU.pdf.

[44] Aitor Martin Rodriguez, *Python3 Script for capturing Bluetooth RSSI on the MK6 OBU*. Mar. 2024. [Online]. Available: aitor.martinrodriguez@uis.no.

[45] *GitHub Copilot - Visual Studio Marketplace*, en-US. [Online]. Available: https://marketplace.visualstudio.com/items?itemName=GitHub.copilot&ssr=false (visited on 05/08/2024).

[46] *EFR Connect BLE Mobile App - Silicon Labs*, en. [Online]. Available: https://www.silabs.com/developers/efr-connect-mobile-app (visited on 04/18/2024).

[47] *Flutter - Build apps for any screen*, en. [Online]. Available: //flutter.dev/ (visited on 04/24/2024).

[48] R. Palankar, *Working with BLE devices in Flutter, Get List of BLE and Connect it.* en-us, Oct. 2023. [Online]. Available: https://protocoderspoint.com/ble-devices-in-flutter-bluetooth-low-energy/ (visited on 05/08/2024).

[49] Google, *Rogaland Rideklubb to Gauselvågen*. [Online]. Available: https://maps.app.goo.gl/sgFfYN84JTD9kFNe6 (visited on 05/13/2024).

[50] *OpenStreetMap*, nb. [Online]. Available: https://www.openstreetmap.org/copyright (visited on 05/14/2024).

[51] L. Jouans, A. C. Viana, N. Achir, and A. Fladenmuller, "Associating the Randomized Bluetooth MAC Addresses of a Device", en, in *2021 IEEE 18th Annual Consumer Communications & Networking Conference (CCNC)*, Las Vegas, NV, USA: IEEE, Jan. 2021, pp. 1–6, ISBN: 978-1-72819-794-4. DOI: 10.1109/CCNC49032.2021.9369628. [Online]. Available: https://ieeexplore.ieee.org/document/9369628/ (visited on 04/27/2024).

Appendix A

Code

Included below is the repository used during the development of our project. The repository can be accessed through GitHub or it can be exported from this pdf: GitHub Repository.7z